AIP | The Journal of Chemical Physics

Interplay between structure and transport properties of molten salt mixtures of ZnCl2–NaCl–KCl: A molecular dynamics study

Venkateswara Rao Manga, Nichlas Swinteck, Stefan Bringuier, Pierre Lucas, Pierre Deymier, and Krishna Muralidharan

Citation: The Journal of Chemical Physics **144**, 094501 (2016); doi: 10.1063/1.4942588
View online: http://dx.doi.org/10.1063/1.4942588
View Table of Contents: http://scitation.aip.org/content/aip/journal/jcp/144/9?ver=pdfcov
Published by the AIP Publishing

Interplay between structure and transport properties of molten salt mixtures of $ZnCl_2$–NaCl–KCl: A molecular dynamics study

Venkateswara Rao Manga,[a] Nichlas Swinteck, Stefan Bringuier, Pierre Lucas, Pierre Deymier, and Krishna Muralidharan
Department of Materials Science and Engineering, University of Arizona, Tucson, Arizona 85721, USA

(Received 12 October 2015; accepted 11 February 2016; published online 1 March 2016)

Molten mixtures of network-forming covalently bonded $ZnCl_2$ and network-modifying ionically bonded NaCl and KCl salts are investigated as high-temperature heat transfer fluids for concentrating solar power plants. Specifically, using molecular dynamics simulations, the interplay between the extent of the network structure, composition, and the transport properties (viscosity, thermal conductivity, and diffusion) of $ZnCl_2$–NaCl–KCl molten salts is characterized. The Stokes-Einstein/Eyring relationship is found to break down in these network-forming liquids at high concentrations of $ZnCl_2$ (>63 mol. %), while the Eyring relationship is seen with increasing KCl concentration. Further, the network modification due to the addition of K ions leads to formation of non-bridging terminal Cl ions, which in turn lead to a positive temperature dependence of thermal conductivity in these melts. This new understanding of transport in these ternary liquids enables the identification of appropriate concentrations of the network formers and network modifiers to design heat transfer fluids with desired transport properties for concentrating solar power plants. © *2016 AIP Publishing LLC.* [http://dx.doi.org/10.1063/1.4942588]

I. INTRODUCTION

There is an on-going search for high operating-temperature heat transfer fluids (HTFs) for an efficient conversion of solar energy in concentrating solar power plants (CSPs).[1–3] The energy conversion efficiency of the CSPs depends on their operating temperature, which in turn is dependent on the thermal stability of the HTFs. In addition to their high boiling/bubble point, the high-temperature HTFs are required to have high heat capacity, high thermal conductivity, low viscosity and low melting/liquidus temperatures. Recent investigations have shown that the $ZnCl_2$–NaCl–KCl ternary liquids remain stable over a wide range of temperatures with favorable thermodynamic properties as required by the high temperature HTFs.[1] Specifically, it was shown that the $ZnCl_2$–NaCl–KCl ternary system demonstrated high thermal stability over a wide range of temperature (250–800 °C) with the heat capacities as demanded by HTFs, providing high performance replacements for currently used systems such as nitrate-based salts.[4] However, barring few studies,[5] the critical transport properties such as viscosity and thermal conductivity of these ternary molten salts have not been well characterized, due to inherent difficulties involved in carrying out experimental measurements, especially at high temperatures. In this regard, using classical molecular dynamics (MD) simulations, the transport properties of $ZnCl_2$–NaCl–KCl ternary liquids are investigated in this study and recommendations for the selection and design of $ZnCl_2$–NaCl–KCl compositions as HTFs for CSPs are provided.

It is known that viscous flow of liquids with underlying network structures exhibits interesting behaviors such as: 1. the breakdown of the Stokes-Einstein (SE) equation,[6] which relates the viscosity to diffusion coefficients of the constituent species and 2. non-Arrhenius temperature-dependence.[6,7] In the case of pure $ZnCl_2$ liquid, which exhibits a network structure predominantly consisting of $ZnCl_4$-tetrahedra[8–10] along with the ability to be easily supercooled to form glass,[7,11,12] while the viscosity is known to show non-Arrhenius behavior,[12,13] its relationship to the underlying diffusion is not yet explored. Furthermore, the addition of monovalent cations such as K^+ or Na^+ (in the form of KCl or NaCl), which serve as network breakers, modify the polymeric network structure of liquid $ZnCl_2$[7,9,14] and consequently, should have a strong effect on the viscosity of the molten mixtures. So far, a comprehensive examination and characterization of the interplay between the network modifiers and the viscosity in $ZnCl_2$ based melts is not available. Towards this end in this study, we characterize the diffusion and viscosity of molten mixtures of network-formers ($ZnCl_2$) and network modifiers (NaCl and KCl) as a function of composition and temperature; such a study will provide important scientific insights into the interplay between structure, composition, and transport in ternary $ZnCl_2$–KCl–NaCl salts.

Further, the extent of network connectivity, resulting from the countervailing effect of the divalent (Zn^{+2}) and the monovalent cations (Na^+ and K^+), should affect the thermal conductivity of the ternary melts. Increasing network connectivity in a network melt can lead to increase in phonon mean free path.[15,16] Hence, an equally important objective of this work will be to provide valuable insights into the interplay between the evolving network character

[a]Author to whom correspondence should be addressed. Electronic mail: manga@email.arizona.edu

of the melts and their thermal conductivity as a function of temperature.

II. METHODOLOGY AND CALCULATION DETAILS

MD simulations were carried out by employing the Born-Huggins-Meyer (BHM) potentials reported by Kumta-Deymier-Risbud (KDR)[17] and Adams and McDonald[18] for $ZnCl_2$ and NaCl/KCl, respectively. In the case of $ZnCl_2$, several different descriptions of classical potentials are available in the literature and among the available potentials, KDR was known to yield a more accurate prediction of the tetrahedral network structure of the liquid.[17] In the investigated $ZnCl_2$–NaCl–KCl molten solutions, dissimilar cation-cation and anion-anion interactions were estimated using different interaction criteria. Lorentz-Berthelot mixing relations were employed for dissimilar cation-cation interactions, which were shown to be accurate in the earlier works.[1,19] In the case of anion-anion interactions in the solutions, the Cl–Cl parameters pertaining to pure liquids of $ZnCl_2$, NaCl, and KCl were weighted based on the atomic fractions of each cation. The chosen potentials in conjunction with the employed mixing relations yielded thermodynamic properties (e.g., heat capacity and enthalpies of mixing) in good agreement with the experimental data.[1] The MD simulations were carried out using the LAMMPS software[20] and employed simulation cells of 8000-10 000 atoms with periodic boundary conditions. It is worth noting that larger MD cells showed identical behavior.

Figure 1 shows the NaCl–KCl–$ZnCl_2$ isothermal section depicting the investigated compositions in this study. The isothermal section is calculated using our NaCl–KCl–$ZnCl_2$ ternary thermodynamic database,[1] which was developed within the CALPHAD (CALculation of PHAse Diagrams) framework. Since the targeted lower limit of the operating temperature for HTFs in CSPs is 250 °C, we chose compositions of NaCl–$ZnCl_2$ and KCl–$ZnCl_2$ binaries that were already in the liquid phase at 250 °C, as the end-members, with a series of intermediate ternary compositions as listed in the Table I. Here CompA and CompF represent the NaCl–$ZnCl_2$ and KCl–$ZnCl_2$ binary compositions while the intermediate compositions, namely, CompB to CompE represent ternary liquids with a gradual increase in the percentage of KCl. It is worth mentioning here that the composition represented by CompC is close to a ternary eutectic composition.

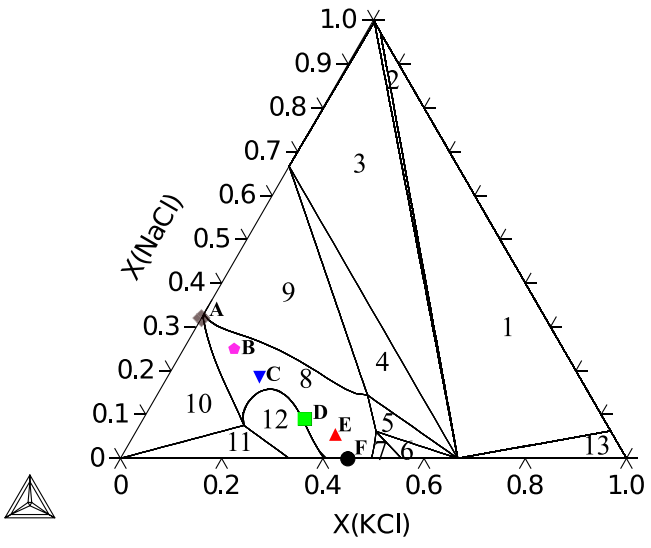

FIG. 1. NaCl–KCl–$ZnCl_2$ isothermal section at 523 K depicting the selected liquid compositions (indicated by the solid symbols) in this study. The liquid region is marked by number 8. Different phase regions indicated by numbers are: 1. SS_NaCl–KCl#1 + SS_NaCl–KCl#2 + K_2ZnCl_4, 2. SS_NaCl–KCl#1 + K_2ZnCl_4, 3. SS_NaCl–KCl#1 + K_2ZnCl_4 + Na_2ZnCl_4, 4. Liquid + K_2ZnCl_4 + Na_2ZnCl_4, 5. Liquid + K_2ZnCl_4, 6. Liquid + $K_5Zn_4Cl_{13}$ + K_2ZnCl_4, 7. Liquid + $K_5Zn_4Cl_{13}$, 8. Liquid, 9. Liquid + Na_2ZnCl_4, 10. Liquid + $ZnCl_2$, 11. Liquid + $ZnCl_2$ + KZn_2Cl_5, 12. Liquid + KZn_2Cl_5, and 13. SS_NaCl–KCl#2 + K_2ZnCl_4. SS_NaCl–KCl#1 and SS_NaCl–KCl#2 indicate the NaCl–KCl solid solutions on the phase diagram. Reproduced with permission from Manga *et al.*, Calphad **46**, 176-183 (2014). Copyright 2014 Elsevier.

For the above identified compositions on the NaCl–KCl–$ZnCl_2$ system, shear viscosity (η), diffusivity (D), and thermal conductivity (κ) of the liquids were obtained by using the Green-Kubo method[21] in conjunction with equilibrium MD simulations.[22] The simulations for these properties were performed under constant energy and volume conditions (NVE) for 2 ns (time-step = 1 fs) using well equilibrated simulation cells that were subjected to isobaric/isothermal conditions at zero pressure and at the temperatures of our interest (600–1050 K). The error bars on the properties were obtained from standard deviation taken over at least 10 different runs at any given temperature and composition.

For thermal conductivity (κ), the time-domain signal generated by MD is the heat flux, **J**(t). **J**(t) is calculated from the fluctuations of per-atom potential and kinetic energies and per-atom stress tensor in a MD simulation at equilibrium. As given by Equation (1), thermal conductivity is averaged with respect to "j" directions for each atomic species,

$$\kappa = \frac{1}{3k_B T^2 V}\int_0^\infty \langle J_j(t).J_j(0)\rangle\, dt. \tag{1}$$

For shear viscosity (η), the time-domain data of interest are the off-diagonal components of the virial pressure tensor (Sxy(t), Sxz(t), and Syz(t)),

$$\eta = \frac{1}{3k_B TV}\int_0^\infty \langle S_{jk}(t).S_{jk}(0)\rangle\, dt. \tag{2}$$

As given by Equation (2), the η is averaged with respect to the off-diagonal components (i.e., j ≠ k). Finally, to calculate the self-diffusion coefficient of all the constituent ionic species in

TABLE I. Melt compositions investigated in this study. The selected compositions are also shown marked on the NaCl–KCl–$ZnCl_2$ isothermal section as shown in Figure 1.

	Composition (mol. %)		
Melt	$ZnCl_2$	NaCl	KCl
CompA	68	32	…
CompB	65	25	10
CompC	63	19	18
CompD	59	9	32
CompE	55	5	40
CompF	55	…	45

the melt (i.e., D_{Na}, D_K, D_{Zn}, D_{Cl}), the velocities of the relevant ionic species, namely, $\mathbf{v}_{Na}(t)$, $\mathbf{v}_K(t)$, $\mathbf{v}_{Zn}(t)$, $\mathbf{v}_{Cl}(t)$, are used in our Green-Kubo post-processing scheme.

The structural characterization of the binary and ternary liquids was carried out using R.I.N.G.S. code,[23] which yielded the pair distribution function and first shell coordination of the different ions in the melt. The analysis of cluster lifetimes and mean-squared displacements (MSDs) of various ions, and the calculations of tetrahedral order parameter in different melts is carried out using our in house code, which is written in MATLAB.

III. RESULTS AND DISCUSSION

A. Structure of the molten salts

As a first step towards characterizing the structure of various liquid compositions, we examine CompC, which represents the ternary composition closest to a ternary eutectic point. Figure 2 shows the pair distribution functions and the first nearest neighbor (NN) coordination shell of the cations of Zn, K, and Na in the CompC melt at 750 K. Here, the cutoff distance for the first NN shell of a given type of ion (Y = Zn or K or Na or Cl) is determined from the first minimum in the weighted sum of Y–X pair distribution functions ($g_{Y-X}(r)$) following Equation (3). In the equation, W_{i-j} represents the composition dependent weighting factors for different atomic pairs in the liquid phase obtained in a fashion similar to Tan *et al.* and Kakinuma *et al.*[24,25]

$$\sum_{X=\mathrm{Zn,K,Na,Cl}} w_{Y-X} g_{Y-X}(r). \tag{3}$$

W_{i-j} for different atomic pairs are calculated by using the equation, $W_{i-j} = {}^{A_i f_i A_j f_j}/_{(\sum A_i f_i)^2}$ (where "A" is the atomic number and "f" is the atomic fraction).[24,25] As shown in Figure 2, the 1st NN radius of Zn (i.e., the cutoff distance

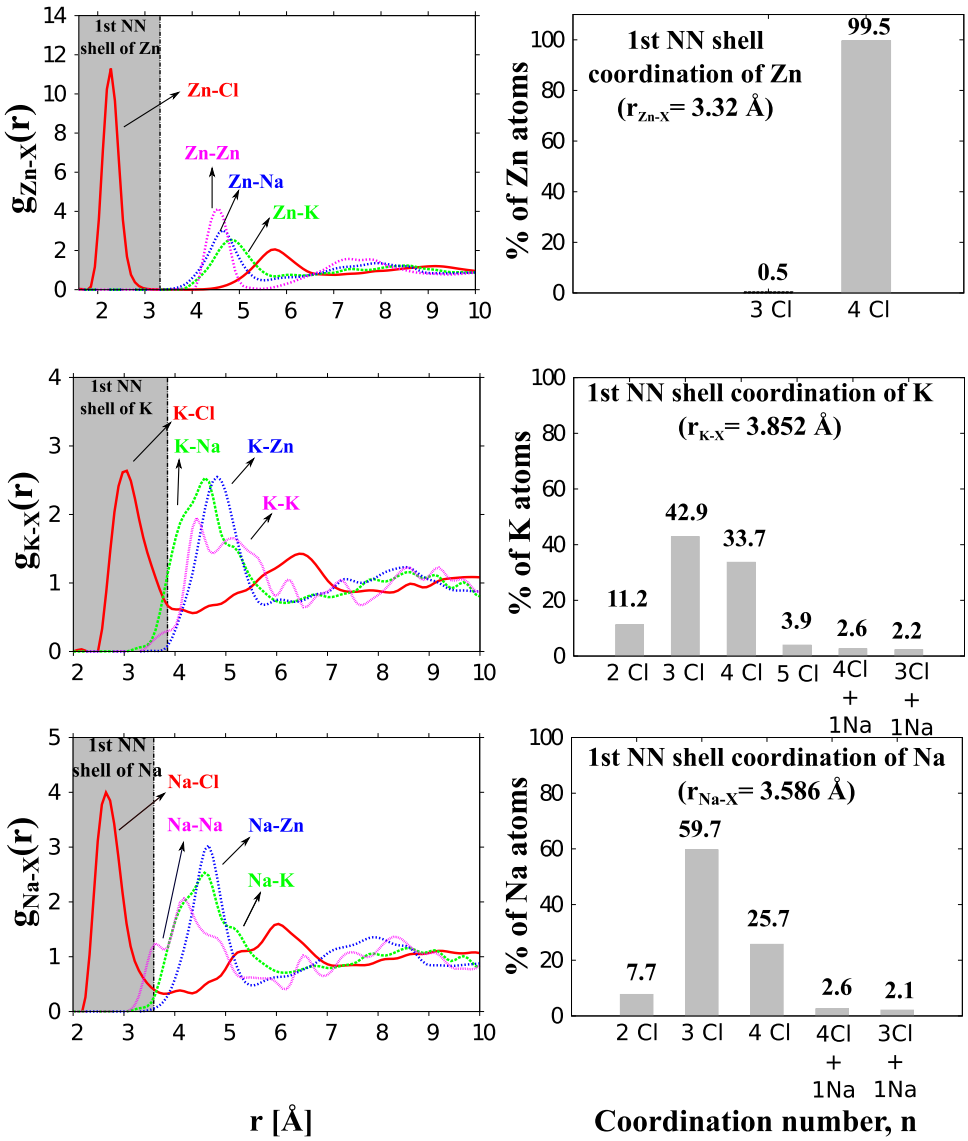

FIG. 2. Pair distribution functions and 1st NN shell coordination of Zn, Na, and K in the ternary melt: 63 mol. % $ZnCl_2$ + 19 mol. % NaCl + 18 mol. % KCl, at 750 K. The shaded area on the pair distribution functions involving a given type of ion indicates the 1st NN shell of that particular ion. The cutoff for the 1st NN shell of each ion is determined from the first minimum in the weighted sum of pair distribution functions ($g_{Y-X}(r)$) following Equation (3). The 1st NN coordination numbers of each ion are then determined within their respective cutoffs.

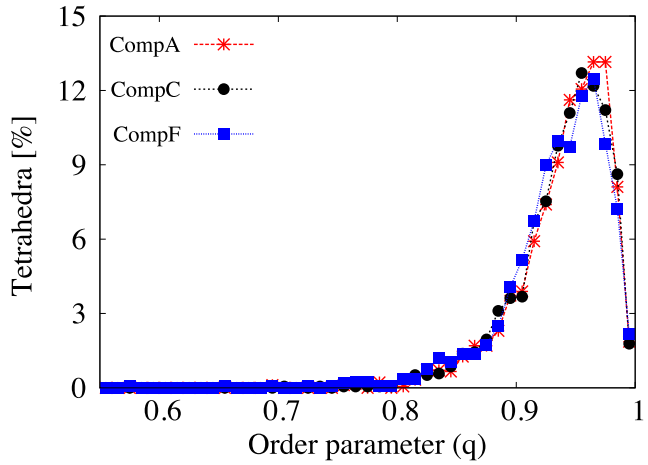

FIG. 3. Distribution of tetrahedral order parameter (q) in three selected melt compositions: CompA, CompC, and CompF. The parameter "q" is calculated by using Equation (4).

for the 1st NN shell of Zn) is 3.32 Å in the ternary liquid of CompC with nearly all Zn ions in the melt exhibiting 4-fold coordination. In addition, the Cl–Zn–Cl bond angle revealed the tetrahedral arrangement of the 4 Cl-ions around each Zn. A tetrahedral order parameter (q) based on the Cl–Zn–Cl bond angles (θ_{jk}) in a given tetrahedron, is calculated using Equation (4).[26] For a perfect tetrahedron (with all the θ_{jk} values being 109.47), the q is equal to "1." The quantified q-parameter in the liquids CompC, CompA, and CompF at 1000 K showed nearly identical distributions (Figure 3). With an average "q" value of ~0.94, clearly the extent of tetrahedrality of $ZnCl_4$-tetrahedra in these liquids is independent of the composition,

$$q = 1 - \frac{3}{8}\sum_{j=1}^{3}\sum_{k=j+1}^{4}\left(\cos\theta_{jk} + \frac{1}{3}\right)^2. \quad (4)$$

In the literature, in an experimental investigation of the structure of KCl–$ZnCl_2$ mixtures employing pulsed neutron diffraction, Allen *et al.*[9] reported that Zn retained its 4-fold coordination, even at high concentrations of KCl in the liquid mixtures. In agreement with their finding, as shown in the figure (Figure 2), 99.5% of Zn ions in the melt are 4-fold coordinated with Cl, while only 0.5% of Zn ions are 3-fold coordinated.

Further, in the CompC liquid, the monovalent cations of K and Na exhibit similar NN environments (Figure 2), consisting of 2-, 3-, and 4-fold coordination, wherein 3-fold coordination occurs as the most prevailing coordination. In the case of the Cl anions, an analysis of the NN coordination afforded the ability to separate the bridging Cl (BC) and non-bridging Cl (NBC) ions. The quantification of bridging (or non-bridging) chlorines in the melt enables the estimation of the connectivity of the tetrahedral network formed by the $ZnCl_4$ units in the liquid. As shown in Figure 4, the anions in the melt exhibit a NN cutoff of 3.05 Å, with ~98% of them bound to at least one Zn. This clearly indicates that the anions remain an integral part of the tetrahedral framework with only a small percentage (~1.2%) solely bound to K and/or Na. Moreover, slightly more than half (54.8%) of the Cl ions were found to be BCs, as ascertained based on the Zn-coordination of the Cl ions. The NBCs, as shown in Figure 4, can be further differentiated as terminal NBCs that are bound to 1Zn only (NBC-1) and non-bridging chlorines of type 2 (NBC-2) that are bound to either 1Zn + 1M or 1Zn + 2M (with M being Na or K). Such a differentiation of total NBCs is done in view of the fact that the evolution and relative proportions of these different types of NBCs as a function of temperature should correlate to the temperature dependence of thermal conductivity and viscosity of the melt (see Section III E).

B. Viscosity-diffusion relationship in the ternary melts

The SE relation is widely used to describe the relationship between self-diffusion coefficients and the viscosity of simple melts and is given by $\eta = {}^{k_B T}/_{6\pi r_i D_i}$, where η is the viscosity of the liquid, D_i is self-diffusion coefficient, k_B is the Boltzmann constant, and r_i is the radius of the diffusing species.[27] Similarly, the Eyring equation ($\eta = {}^{k_B T}/_{\alpha_i D_i}$, where α_i is jump distance), assuming the same thermally activated process responsible for the diffusion and viscosity, describes the D–η relationship based on transition state theory.[28,29] While both these equations are essentially the same formula, α_i in the Eyring equation is the jump distance and is also interpreted as the diameter of the diffusing species;[30] the Eyring and SE just differ by a constant factor. The usefulness of these SE/Eyring equations in different types of liquids (i.e., with simple structures or polymeric network-structures) and in a wide range of conditions (i.e., temperature and pressure) is

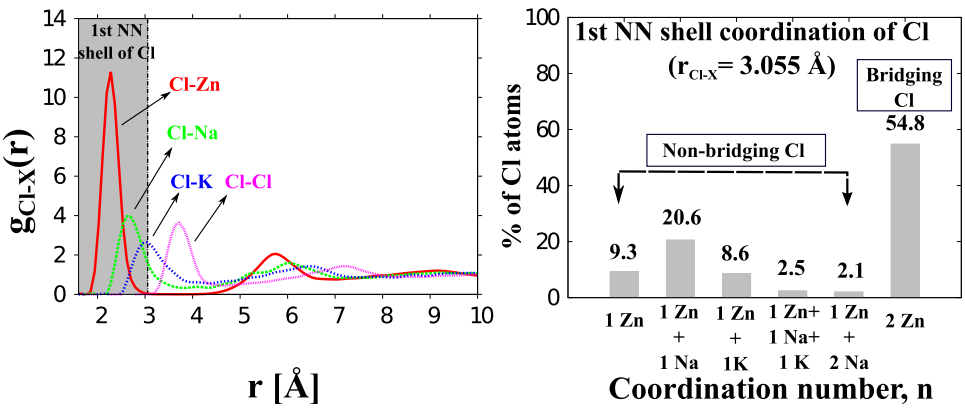

FIG. 4. First nearest neighbor shell of Cl in the ternary melt: 63 mol. % $ZnCl_2$ + 19 mol. % NaCl +18 mol. % KCl, at 750 K. The shaded area on the pair distribution functions indicates the 1st NN shell of Cl. The cutoff for the 1st NN shell of Cl (r_{Cl-X}) is found to be 3.05 Å (determined from the first minimum in the weighted sum of pair distribution functions following Equation (3)) and the 1st NN coordination numbers of Cl are determined within this cutoff.

a subject of intense research. In the case of silicate melts with tetrahedral network-structures, similar to $ZnCl_2$ melts, the Eyring equation was found to be more reliable and useful to relate the viscosity and diffusion.[30,31] Such a validation of the Eyring model in silicate melts further led to the atomistic insight into the thermally activated transport mechanism; "Si" and "O" in the melt are transported cooperatively, in the form of "molecular units."[30] In light of these findings, we examined the usefulness of SE and Eyring models to relate the diffusion of different types of ions and viscosity in the NaCl–KCl–$ZnCl_2$ melts as a function of composition.

Figure 5 shows the plot of the ratio $\alpha_i (= {}^{k_BT}/_{\eta D_i})$ as a function of temperature for every ion in all the selected melt compositions. Clearly, as shown in the figure, in none of melts (i.e., CompA to CompF) the diffusion coefficient of Zn exhibits a valid SE or Eyring relationship. Such a failure of SE in network-forming and glass-forming liquids in the vicinity of glass transition temperature is well known.[6,27,32] Decoupling of the diffusion and structural relaxation (i.e., viscosity) in these network-forming liquids with underlying spatial and temporal heterogeneities in transport is evident from the breakdown of the SE.[33] Interestingly, among all the different types of ions, when $ZnCl_2 < 63$ mol. % and as we increase the KCl composition (CompC to CompF), only the monovalent K ion demonstrates a constant α_K (~3.3-6.3 Å: see Table II) across the entire range of temperature. Within the SE relationship, this yields an unphysical ionic radius of ~0.27 Å for the diffusing K. However, within the Eyring model, this α_K gives a jump distance of 3.3-6.3 Å for the thermally activated diffusion of K. Specifically, in CompC, the mean α_K (= 3.3 Å)—though larger than the diameter of K^+ (~2.74 Å)[34]—is smaller than the 1st NN radius of K, and could be interpreted as the atomic jump distance of K. In other words, in CompC the viscosity and the diffusion of K are dictated by the same atomic jump process of K. But in the case of CompF-CompD, the mean α_K (= 5-6.3 Å), which is larger than the 1st NN radius of K, indicates a possible cooperative transport of "molecular units" of K and Cl. It is worth recalling a previous observation that in CompC at 750 K (Figure 4), while only 1.2% of total Cl ions are solely bound to K/Na, ~34% of Cl-ions form the NBC of type 2 (NBC-2). Thus, a cooperative transport mechanism involving "molecular units," as observed in silicate melts,

TABLE II. Calculated mean of α_K from the Stokes-Einstein like relation ($\alpha_K = \frac{k_BT}{\eta D_K}$) between the diffusion coefficient of K and the viscosity of the liquids of CompC to CompF. In liquids with Comp A and CompB, none of the ions exhibit a constant value of the ratio ($\frac{k_BT}{\eta D_K}$) as a function of temperature and so are not listed in the table.

Melt	α_K (Å)
CompC	3.3 ± 0.2
CompD	6.3 ± 1.4
CompE	5.1 ± 0.5
CompF	5.0 ± 0.9

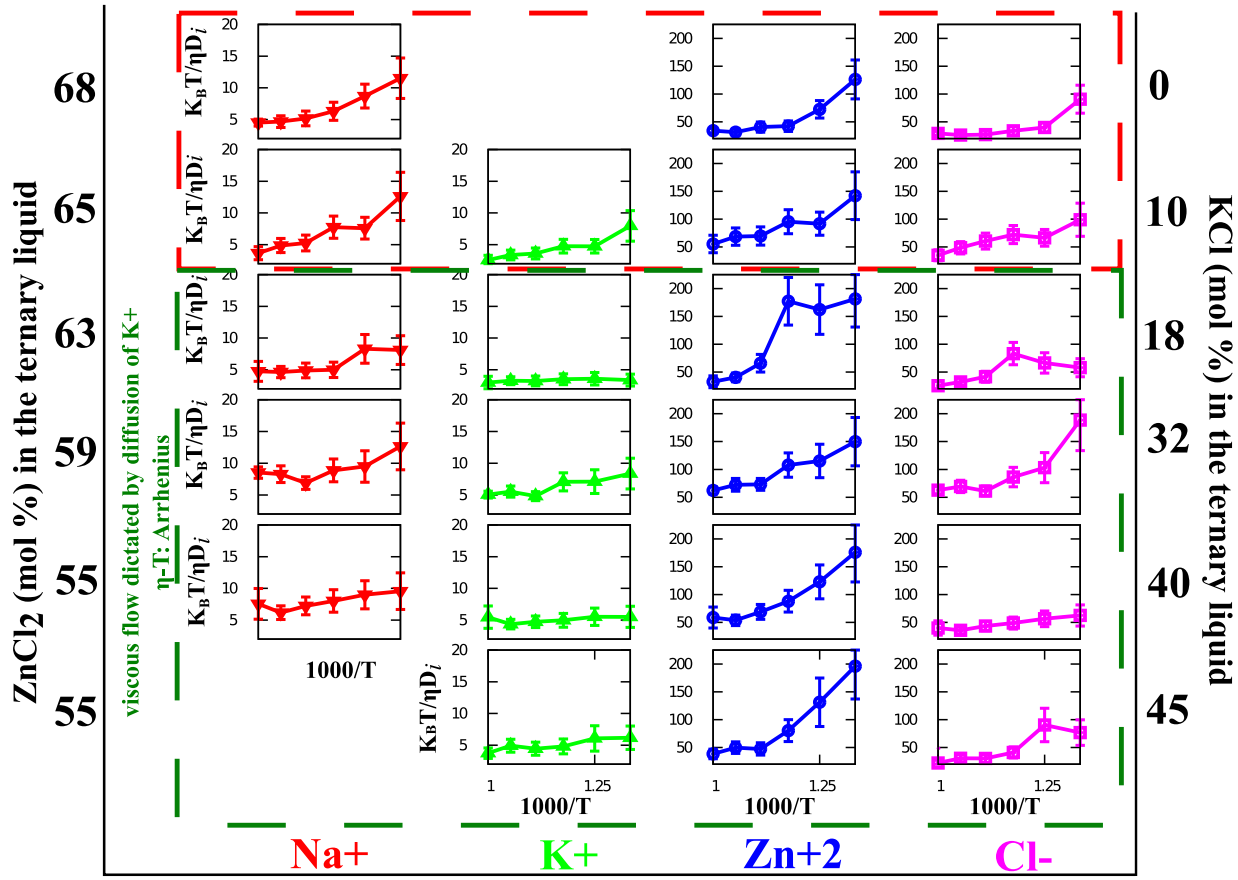

FIG. 5. Viscosity–diffusivity relationship in the NaCl–KCl–$ZnCl_2$ liquids. The ratio ${}^{k_BT}/_{\eta D_i}$ vs T for each ion in the selected melt compositions—CompA to CompF. The ratio should remain constant as a function of temperature if SE or Eyring relations is valid.

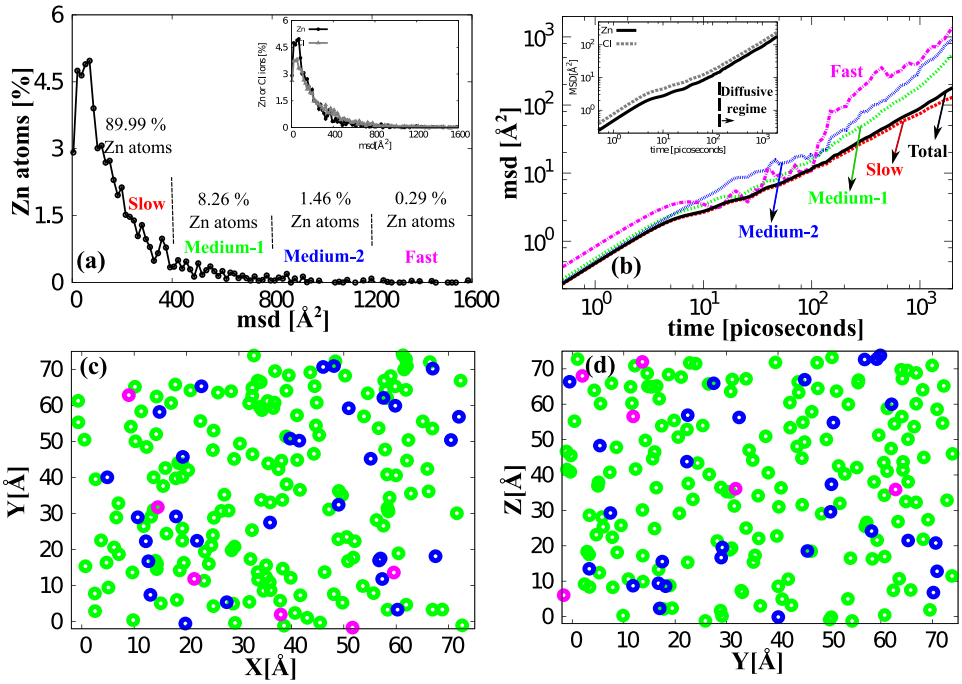

FIG. 6. Heterogeneities in diffusion of network-former (Zn) in the CompC liquid at 1000 K. (a) the distribution of MSD of individual Zn ions after 2 ns. The Zn ions are classified as "Slow," "Medium-1," "Medium-2," and "Fast" moving depending on their MSD values at the end of the simulation run (2 ns). Inset shows the comparison of distributions of individual MSD of Zn and Cl ions after 2 ns. (b) log-log plot of the average MSD as a function of time of "Slow," "Medium-1," "Medium-2," and "Fast" moving Zn ions. The black solid line (marked as "Total") is the ensemble average of all Zn ions in the melt. Inset shows the ensemble averages of MSD of Zn and Cl ions as a function of time. The dashed vertical line approximately marks the beginning of linear diffusive regime on the MSD of Cl. (c, d) XY and YZ projections of spatial distribution of "Medium-1," "Medium-2," and "Fast" Zn ions at t = 2 ns.

could be responsible for the observed α_K. Such a transport of molecular units of K and Cl, also indicate a possible higher mean-squared displacements for Cl in comparison to the network-forming Zn (see Section III C).

Another interesting outcome of this analysis, as shown in Figure 5, is that the ratio, α_{Na} (pertaining to Na ions) behaves differently in comparison to K. In none of the liquids, except in CompE, α_{Na} remains constant with temperature. Within the limits of the error bars, the α_{Na} remains constant only in the liquid with 5 mol. % NaCl (CompE) and gets a mean value of ~7.3 Å. Within SE relationship, the α_{Na} of ~7.3 Å yields a radius of 0.39 Å for the diffusing Na and, the obtained radius is too small for the radius of Na^+. This high value for $\boldsymbol{\alpha}_{Na}$ is nearly twice the 1st NN radius of Na.

C. Mean-squared displacements and cluster lifetimes in the melts

In order to further analyze the observed differences between different types of cations in obeying the Eyring expression, we examined the MSDs of different types of ions in CompC liquid. Temporal and spatial heterogeneities in the MSDs of the network former (Zn^{+2}) in the CompC liquid at 1000 K are shown in Figure 6. The distribution of individual MSD of all the Zn ions in the melt after 2 ns is shown in the figure (Figure 6(a)). While nearly 90% of the total Zn ions, which are labeled as slow moving, exhibited MSD ≤ 400 $Å^2$, the top 10% showed MSD distributed between 400 and 1600 $Å^2$. A further split-up of this top-10% into "Medium-1," "Medium-2," and "Fast" moving Zn ions is also shown on the figure. Figure 6(b) shows the log-log plot of the average MSD of Zn ions from different categories (i.e., Slow, Medium-1, Medium-2, and Fast) as a function time; clearly, within the diffusive regime, the time-dependence of MSD of medium and fast moving Zn ions reveals the temporal heterogeneities in the diffusion of the network former. The diffusive regime (with preceding ballistic and "cage" regimes) for both Zn and Cl began after approximately 100 and 150 ps (inset Figure 6(b)), respectively. Figures 6(c) and 6(b) shows the spatial distribution of the medium and fast moving Zn ions after 2 ns (the slow moving Zn ions are not shown for clarity). These temporal and spatial heterogeneities in the mean-squared displacement of Zn ions are indicative of the "glass dynamics" in these tetrahedral liquids.

In the case of monovalent cations, as shown in Figure 7(a), the distributions of individual MSD of K and Na ions in the CompC liquid at 1000 K after 2 ns are nearly identical. A comparison of the average MSD of K and Na ions as a function

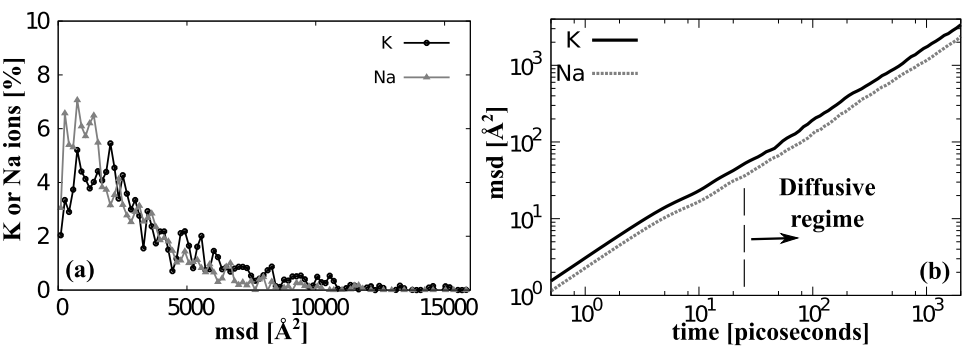

FIG. 7. MSD of the network modifiers (K and Na) in the CompC liquid at 1000 K (a) distribution of MSD of individual monovalent cations after 2 ns; (b) log-log plot of the average MSD of K and Na as a function of time. The dashed vertical line approximately marks the beginning of linear diffusive regime on the plot.

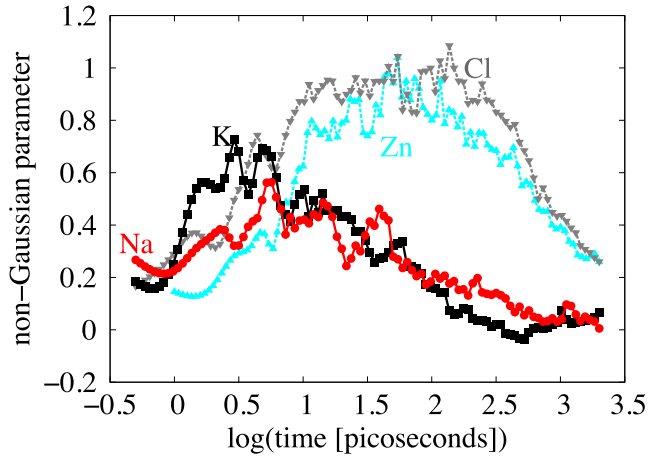

FIG. 8. Non-Gaussian parameter, N(Δt) of K, Na, Zn, and Cl as a function of time in CompC liquid at 1000 K.

of time (Figure 7(b)) shows that K is faster than Na and is the fastest moving ion in the liquid. Further, the log-log plot also reveals that, in comparison to Zn or Cl, the diffusive regime begins early for the monovalent cations (after approximately 25 ps).

In order to further elucidate the observed heterogeneities in diffusion in these tetrahedral liquids, we calculated non-Gaussian parameter ($N(\Delta t) = \frac{3\langle \Delta r(\Delta t)^4 \rangle}{5\langle \Delta r(\Delta t)^2 \rangle^2} - 1$)—a metric that is reported in the literature[35,36] to quantify the heterogeneities. In the absence of "glassy dynamics" or heterogeneities in MSDs, the N(Δt) is zero. The calculated N(Δt) of K, Na, Zn, and Cl in the CompC liquid at 1000 K is shown in Figure 8. As shown in the figure, both Zn and Cl exhibit similar N(Δt), attaining peak values at times 45 ps and 140 ps, respectively. Similarly, both K and Na exhibit nearly identical N(Δt), which are clearly different from those of the divalent ions. Clearly, the times corresponding to the peak values of N(Δt) are greater for the divalent ions than for the monovalent cations and indicate relatively higher relaxation time scales on the $ZnCl_4$-tetrahedral units. Further, a relatively higher N(Δt) on the divalent ions also indicate a greater degree of heterogeneities in their dynamics in comparison to the network modifiers (i.e., K and Na).

Interestingly, while both Na and K exhibit nearly similar behavior in terms of the distribution of MSD at 1000 K, only K exhibits the Eyring relationship (as seen in Section III B). Thus, as a next step towards understanding the observed difference between Na and K in the Eyring relationship, we performed the lifetime analysis of different tetrahedral clusters and tetrahedron-M (M = Na or K) bonds. Such an analysis can reveal the differences between K and Na in terms of their affinity towards the tetrahedral network.

The distribution of lifetimes of individual $ZnCl_4$-tetrahedra and 5-tetrhedra clusters are shown in Figure 9. Lognormal distribution of the lifetimes of these tetrahedral clusters is obtained with some $ZnCl_4$-tetrahedra exhibiting lifetimes even longer than 100 ps. In the cluster-lifetime distributions, the time at which the cumulative percentage of population reaches 50 is defined as "t_{50}." Clearly, the lifetime of 5-tetrahedra clusters as expressed by its t_{50} (= 7–9 ps) is smaller by a factor ∼4 in comparison to the lifetime of individual $ZnCl_4$-tetrahedra (with t_{50} =∼ 35 ps). However, the K or Na bonding with the $ZnCl_4$-tetrahedral units exhibits relatively smaller lifetimes; t_{50} of the tetrahedron-K and tetrahedron-Na binding is ∼2 ps and ∼3.25 ps, respectively. Most importantly, in comparison to K, Na showed longer average-lifetime in its binding with the tetrahedral network. The relatively slower diffusion (smaller MSD in Figure 7) and the longer lifetimes of tetrahedron-Na bonds indicate that Na is more "tightly" bound to the network than K. This difference in the binding to the network could be responsible for the observed difference between K and Na in the Eyring relationship.

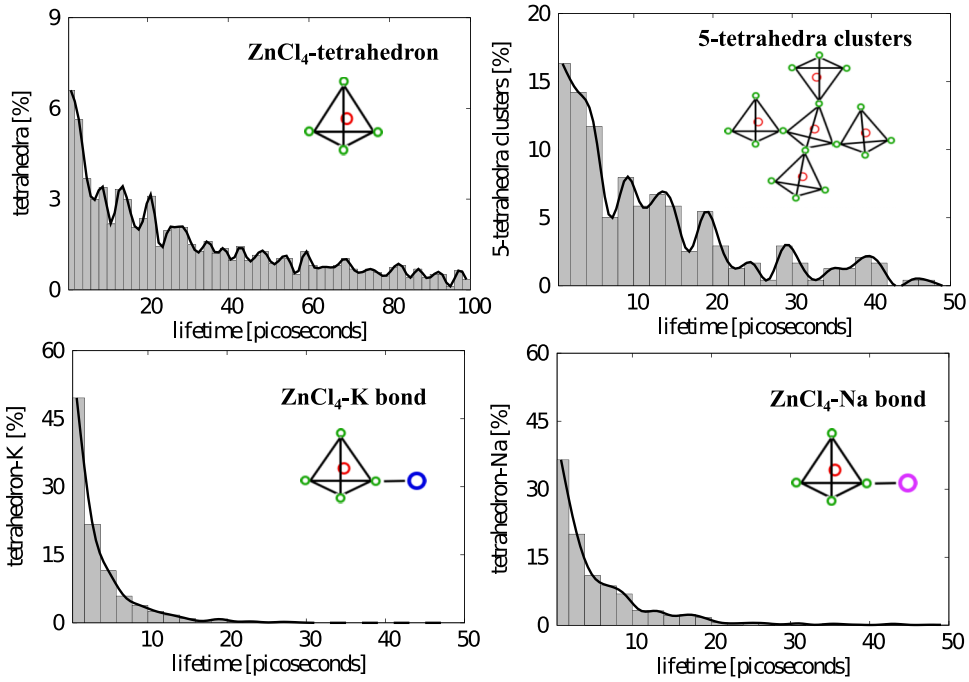

FIG. 9. Lifetime distribution of clusters of different sizes in CompC liquid at 1000 K. (a) Lifetimes of individual $ZnCl_4$-tetrahedra. (b) Lifetimes of 5-tetrahedra clusters. (c) Lifetimes of tetrahedron-K binding and (d) lifetimes of tetrahedron-Na binding.

D. Temperature dependence of viscosity

As shown above (in Section III B), in light of the validity of Eyring model—i.e., with the thermally activated migration of K relating the diffusion and viscosity—the temperature dependence of the viscosity of the KCl-rich liquids (CompC to CompF) are described by an Arrhenius equation (Equation (5)),

$$\eta\,(T) = \eta_B \exp\left(\frac{B}{RT}\right), \tag{5}$$

where B represents an activation energy term and η_B is the pre-exponential term. Arrhenius fits of the viscosities of the liquids (CompC to CompF) along with the estimated viscosities using the diffusion coefficient (D_K) and the mean jump-distance (α_K: shown in Table II) within the Eyring relationship are shown in Figure 10. Clearly, Eyring expression provides a useful relationship to predict viscosity of the KCl-rich liquids (CompC to CompF) from the diffusion coefficients of K. The activation energies (B) obtained for the viscous flow are listed in Table III. In contrast, at the other end of the composition spectrum, namely, for CompA and CompB, as noted earlier, an Eyring relationship is not applicable, indicating that these liquids typify characteristics of fragile liquids.[6,37] In light of the observed breakdown of the Eyring equation, we employed a non-Arrhenius Vogel-Tamman-Fulcher (VTF) equation (Equation (6)) to describe the temperature dependence of viscosity (Figure 11) of these $ZnCl_2$ rich KCl-deficient liquids.

$$\eta\,(T) = \eta_A\sqrt{T}\exp\left(\frac{A}{T - T_0}\right), \tag{6}$$

where T_0 is the ideal glass transition temperature, A is equal to activation energy divided by gas constant (R), and η_A is pre-exponential term, both of which are listed in Table III. It is worth mentioning here that within the limits of the error bars, the viscosity of these melts could also be fit with an Arrhenius equation with similar goodness of fit. Nitta *et al.*[5] have reported a VTF fit of their experimentally measured viscosity for a ternary liquid with 60 mol. % $ZnCl_2$ + 20 mol. % NaCl + 20 mol. % KCl, in a narrow temperature range of 200-300 °C. Though the experimental composition is different from the CompA or CompB in this work, a comparison of the fit parameters—the T_0, A, and η_A—reveals a close agreement with the experimentally reported values, confirming the accuracy and applicability of this work.

TABLE III. Parameters from the Arrhenius and VTF fits of viscosity data of the liquids (shown in Figures 10 and 11). The composition of the ternary melt in the studies of Nitta *et al.*[5] is 60 mol. % $ZnCl_2$ + 20 mol. % NaCl + 20 mol. % KCl.

Arrhenius fit		
Liquid	η_B (P)	B (J/mol)
CompC	1.84×10^{-3}	1987.4
CompD	0.54×10^{-3}	2785.9
CompE	0.40×10^{-3}	2882.2
CompF	1.28×10^{-3}	1868.6

Vogel-Tamman-Fulcher fit			
Liquid	η_A (P $K^{-1/2}$)	A (K)	T_0 (K)
CompB	1.36×10^{-3}	1081.6	270.8
CompA	1.07×10^{-3}	984	278.8
Nitta *et al.*[5,a]	1.23×10^{-4}	1210	283

[a]The composition is different from CompA or CompB.

E. Thermal conductivity of the liquids

The network character and the length of the polymeric tetrahedral-chains in network-forming liquids have been shown to affect the thermal conductivity of the melts.[15,16] Specifically, the fraction of non-bridging anions is shown to adversely affect the thermal phonon transport.[38] In this context, a detailed characterization of NBC in terms of their

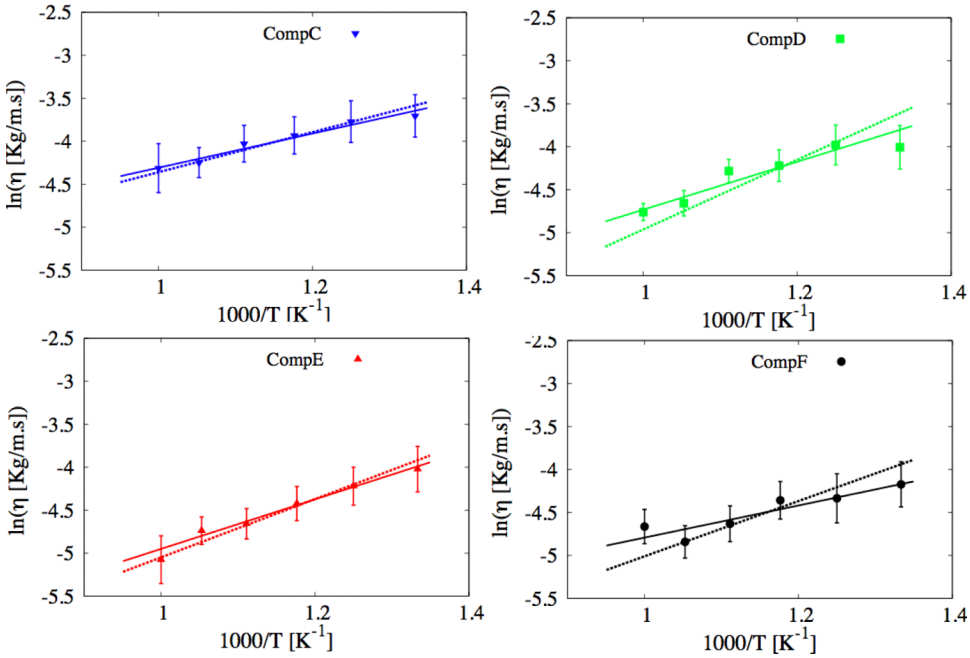

FIG. 10. Temperature dependence of viscosity of the NaCl–KCl–$ZnCl_2$ ternary liquids, CompC to CompF (see Figure 1 and Table I). The symbols are the MD-predicted viscosity data and the solid line is the Arrhenius fit of the MD-predicted data. The dashed line is the estimated viscosity from the diffusion coefficient of K and the mean α_K (shown in Table II), using Eyring relationship ($\eta = \frac{k_B T}{\alpha_K D_K}$).

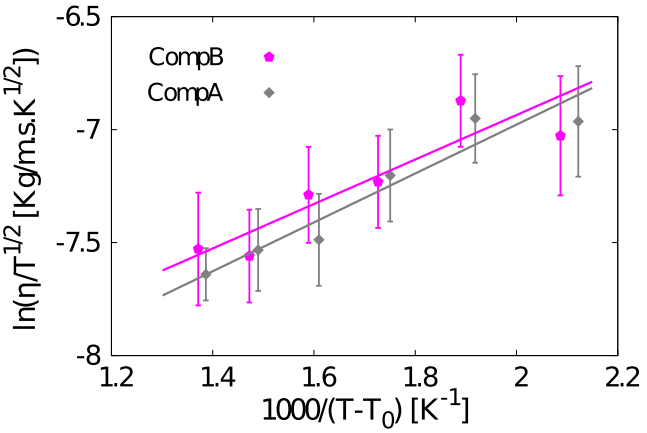

FIG. 11. Temperature dependence of viscosity of the NaCl-KCl-$ZnCl_2$ ternary liquids of CompA and CompB (see Figure 1 and Table I). The solid line is the VTF fit of the viscosity of the melts and the symbols are MD predicted data.

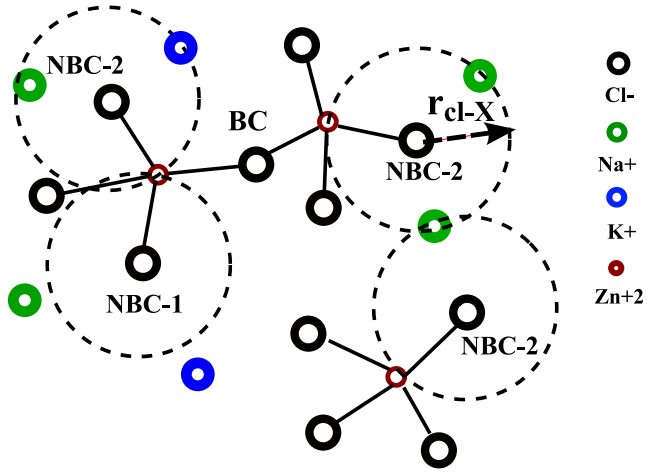

FIG. 13. Depiction of BC, NBC-1, and NBC-2 in the tetrahedral network. The cutoff for the 1st NN shell of Cl (r_{Cl-X}) is determined from the first minimum in the weighted sum of pair distribution functions (following Equation (3)) and the 1st NN coordination numbers of Cl are determined within this cutoff.

NN coordination and their relation to the thermal conductivity in the chloride melts is presented in this section.

Figure 12 shows the thermal conductivity of the $ZnCl_2$-based liquids as a function of temperature. While linear fits of the data, as shown in the figure, reveal a positive temperature dependence of the thermal conductivity in all the liquids except CompA, within the limits of the error bars, the fits are reliable only for CompD to CompF. In the case of CompA to CompC, the trends shown by the fit lines are not meaningful due to the error bars on the data. As mentioned earlier, in network-forming oxide melts, positive temperature dependence of thermal conductivity was attributed to increasing tetrahedral chain length, as given by decreasing non-bridging oxygens per tetrahedron (NBO/T), with increasing temperature.[15] On a similar note, we quantified the temperature-dependent evolution of not only the percentage of NBC and BC but also of the different types of NBC present in the melts. As shown in Figure 13, unlike terminal NBC (i.e., NBC-1), non-bridging chlorine of second type (i.e., NBC-2) can exhibit

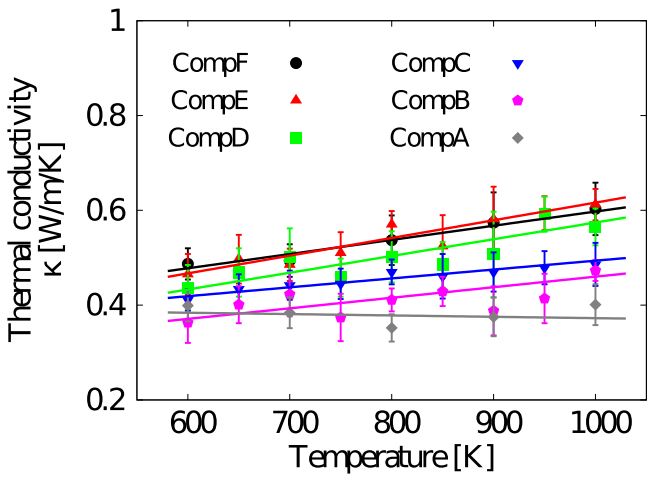

FIG. 12. Thermal conductivity of the NaCl–KCl–$ZnCl_2$ melts as a function of temperature. The solid lines are the linear fits of the MD predicted thermal conductivity. Thermal conductivity of the melts, CompD, CompE, and CompF, exhibits positive temperature dependence.

K- or Na-mediated connectivity with other chains/tetrahedra. As a result, the thermal resistance for the transport of phonons from chain to chain could be smaller at NBC-2 in comparison to the resistance at NBC-1. It is worth mentioning here that a further separation of NBC-2 into different types based on their 1st NN monovalent cations is also possible.

Figure 14 shows the temperature dependence of BC and NBC in all the investigated liquids (CompA to CompF) on the NaCl–KCl–$ZnCl_2$ ternary. Clearly, in all the liquids, the populations of BC and total NBC remain nearly unchanged with varying temperature. However, the populations of NBC-1 and NBC-2 show significant temperature-dependence. Most importantly, in the KCl-rich liquids (CompD-CompF), the NBC-1 shows a huge decrease with increasing temperature while the opposite is true for NBC-2. Such an increase in NBC-2 with temperature points to an increase in the K- (or Na-) mediated connectivity between different tetrahedral chains. This finding explains and correlates well with the positive temperature dependence of thermal conductivity of the CompD-CompF liquids. The ratio, NBC-1/NBC-2, plotted against temperature (Figure 15) also reveals the temperature dependence of the extent of K- (or Na-) mediated connectivity between different tetrahedral chains. In contrast, the liquids with high $ZnCl_2$-concentration (≥63 mol. %)—i.e., CompA-CompC—show a different behavior in terms of relative proportions and the temperature dependence of NBCs: 1. the population of NBC-1 is significantly lower than NBC-2 at all temperatures and 2. the ratio, NBC-1/NBC-2, nearly remains constant (inset in Figure 15). In other words, in the CompA-CompC liquids, the extent of network connectivity nearly remains unchanged within the temperature range of interest (600-1000 K). Thus, as evident from the discussion, a significant increase in network connectivity via K-mediation leads to the positive temperature-dependence of thermal conductivity in the CompD-CompF liquids. It is also clear from this analysis that even while the percentage of the total NBC remained unchanged, the changes in the relative proportions of NBC-1 and NBC-2 affected the network

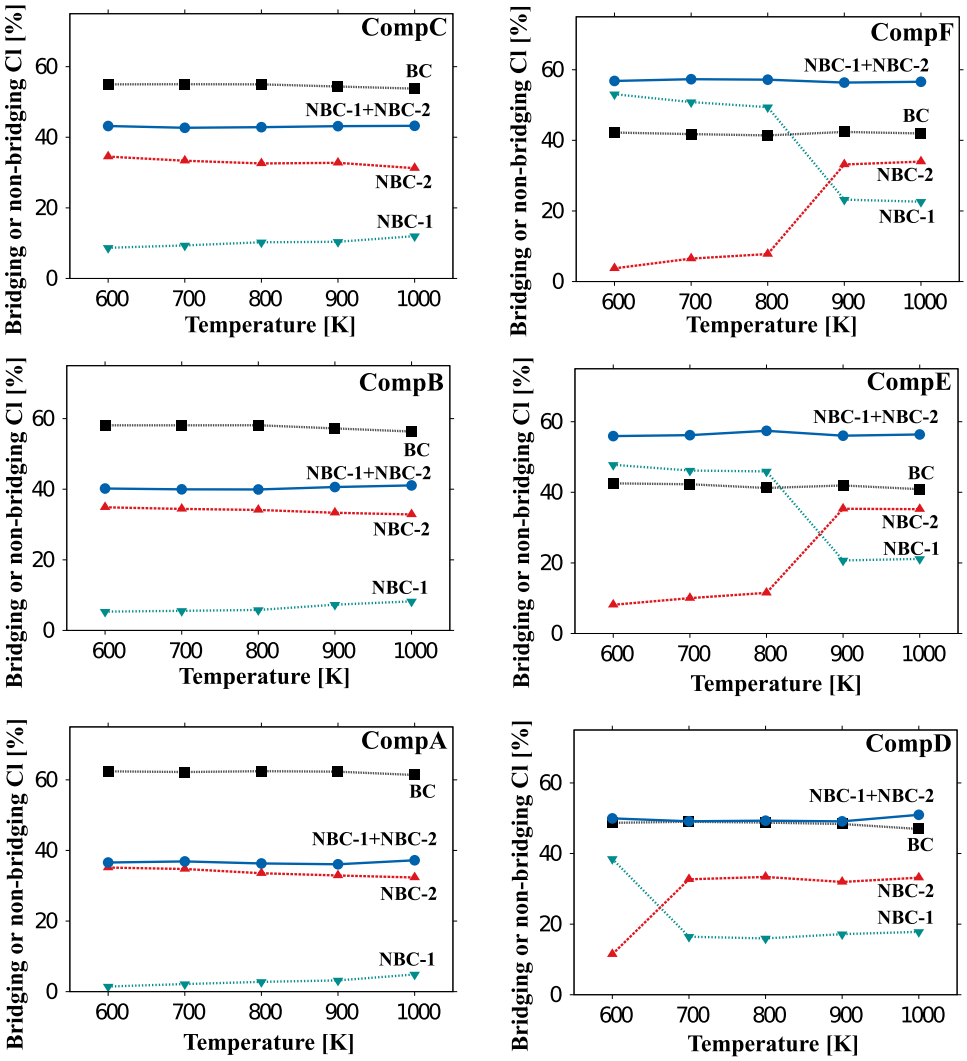

FIG. 14. Temperature dependence of populations of BC and NBC in liquids of CompA to CompF (see Figure 1 and Table I). The BC and NBC of different types (NBC-1 and NBC-2) are depicted in Figure 13.

connectivity and the phonon mean free path. Thus, extending this finding to oxide melts, a further separation of the non-bridging oxygens into NBO-1 and NBO-2 will lead to an improved understanding of the interplay between the network connectivity and thermal conductivity.

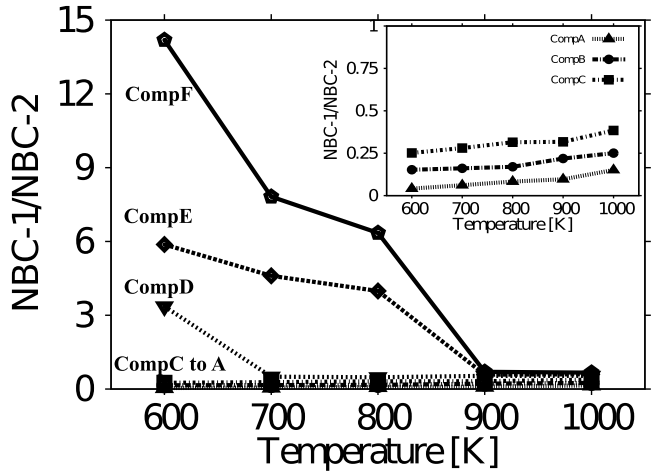

FIG. 15. Ratio of NBC-1 to NBC-2 in the liquids (CompA to CompF) as a function of temperature. Inset shows the enlarged view of the ratio in the liquids, CompA to CompC.

Based on the above results and discussion, it is clear that between the two monovalent network modifiers (K and Na) in the $ZnCl_2$-based molten salts, K leads to a better combination of low viscosity and high thermal conductivity of the liquid. In terms of the transport properties, HTFs are required to have low viscosities and high thermal conductivities for higher operating performance in CSPs. In view of these properties, liquids with higher percentages of KCl (i.e., compositions close to the KCl–$ZnCl_2$ binary composition) should be the preferred HTF compositions. However, as mentioned earlier, the overall performance of heat transfer fluids depends on a combination of various thermodynamic (e.g., heat capacity) and transport properties (viscosity and thermal conductivity) in addition to their ability to operate at very high temperatures while exhibiting low melting/liquidus points and future work will focus on identifying compositions with optimal thermochemical and transport properties as demanded by the high-temperature HTFs.

IV. SUMMARY

In this work, for the first time, we have undertaken classical MD simulations to investigate the interplay between the structure, composition, and transport properties of

NaCl–KCl–$ZnCl_2$ liquids. The countervailing effect of the network-forming (Zn) and network-modifying (Na and K) ions in these liquids leads to a strong composition dependent behavior in the viscosity of the liquids. At high $ZnCl_2$ concentrations (>63 mol. %), it was found that the Stokes-Einstein/Eyring relationship breaks down indicating a predominant network character in the underlying structure of the liquid. Hence, the temperature dependence of the viscosity of the liquids (with $ZnCl_2$ >63 mol. %) was described by a non-Arrhenius VTF equation. However, with $ZnCl_2$ concentrations ≤63 mol. %, the viscosity of the liquids is related to the diffusion coefficient of the monovalent cation K^+, via an Eyring equation. Thus, in light of the observed Eyring relationship, an Arrhenius equation was employed to fit the viscosity of these liquids with non-network character.

An equally interesting outcome of this study is that the $ZnCl_2$-based liquids with higher percentages of KCl exhibit a positive temperature dependence of thermal conductivity. A detailed characterization of non-bridging chlorines, which occur due to the presence of the K ion revealed that the ratio of two distinct non-bridging chlorine types could be directly correlated to the observed trends in the positive temperature dependence of thermal conductivity.

In summary, on the identified $ZnCl_2$–NaCl–KCl ternary liquid space, the KCl-rich liquids are found to offer an optimal combination of low viscosity and high thermal conductivity as demanded by the HTFs that can operate in a huge range of temperatures (250–800 °C).

ACKNOWLEDGMENTS

We acknowledge the financial support from the US Department of Energy (DoE)—multi-university research Grant No. DE-EE0005942 under the US DoE sunshot program.

[1]V. R. Manga, S. Bringuier, J. Paul, S. Jayaraman, P. Lucas, P. Deymier, and K. Muralidharan, Calphad **46**, 176 (2014).
[2]A. K. Starace, J. C. Gomez, J. Wang, S. Pradhan, and G. C. Glatzmaier, J. Appl. Phys. **110**, 124323 (2011).
[3]J. W. Raade and D. Padowitz, J. Sol. Energy Eng. **133**, 031013 (2011).
[4]K. Coscia, T. Elliott, S. Mohapatra, A. Oztekin, and S. Neti, J. Sol. Energy Eng. **135**, 021011 (2013).
[5]K. Nitta, T. Nohira, R. Hagiwara, M. Majima, and S. Inazawa, Electrochim. Acta **54**, 4898 (2009).
[6]M. Bouhadja, N. Jakse, and A. Pasturel, Mol. Simul. **40**, 251 (2013).
[7]L. E. Pedersen, *Viscosity, Structure and Glass Formation in the AlCl 3 -ZnCl 2 System* (Norges Teknisk-Naturvitenskapelige Universitet, 2001).
[8]D. A. Allen, R. A. Howe, N. D. Wood, and W. S. Howells, J. Chem. Phys. **94**, 5071 (1991).
[9]D. A. Allen, R. A. Howe, N. D. Wood, and W. S. Howells, J. Phys.: Condens. Matter **4**, 1407 (1992).
[10]S. N. Yannopoulos, A. G. Kalampounias, A. Chrissanthopoulos, and G. N. Papatheodorou, J. Chem. Phys. **118**, 3197 (2003).
[11]A. J. Easteal, J. Chem. Phys. **56**, 4231 (1972).
[12]M. V. Susic and S. V. Mentus, J. Chem. Phys. **62**, 744 (1975).
[13]T. Ejima, T. Yoko, and K. Nakashima, J. Jpn. Inst. Met. **41**, 86 (1977).
[14]B. Moyer and E. Section, Inorg. Chem. **21**, 3552 (1982).
[15]Y. Kim and K. Morita, J. Am. Ceram. Soc. **98**, 1588 (2015).
[16]K. C. Mills, ISIJ Int. **33**, 148 (1993).
[17]P. N. Kumta, P. A. Deymier, and S. H. Risbud, Physica B **153**, 85 (1988).
[18]D. J. Adam and I. R. McDonald, J. Phys. C: Solid State Phys. **7**, 2761 (1974).
[19]F. T. Smith, Phys. Rev. A **5**, 1708 (1972).
[20]S. Plimpton, J. Comput. Phys. **117**, 1 (1995).
[21]D. Frenkel and B. Smit, *Understanding Molecular Dynamics Simulation from Algorithms to Applications* (Academic Press, New York, 2002).
[22]D. C. Rapaport, *The Art of Molecular Dynamics Simulation*, 2nd ed. (Cambridge University Press, 2004).
[23]S. Le Roux and P. Jund, Comput. Mater. Sci. **49**, 70 (2010).
[24]J. Tan, G. Wang, Z. Y. Liu, J. Bednarčík, Y. L. Gao, Q. J. Zhai, N. Mattern, and J. Eckert, Sci. Rep. **4**, 3897 (2014).
[25]F. Kakinuma, S. Hosokawa, H. Ikemoto, S. Kohara, and Y. Tsuchiya, J. Phys.: Conf. Ser. **502**, 012029 (2014).
[26]J. R. Errington and P. G. Debenedetti, Nature **409**, 318 (2001).
[27]S. R. Becker, P. H. Poole, and F. W. Starr, Phys. Rev. Lett. **97**, 055901 (2006).
[28]H. Eyring, J. Chem. Phys. **4**, 283 (1936).
[29]D. Tinker, C. E. Lesher, G. M. Baxter, T. Uchida, and Y. Wang, Am. Mineral. **89**, 1701 (2004).
[30]D. Tinker and C. E. Lesher, Am. Mineral. **86**, 1 (2001).
[31]N. Shimizu and I. Kushiro, Geochim. Cosmochim. Acta **48**, 1295 (1984).
[32]M. Bauchy, B. Guillot, M. Micoulaut, and N. Sator, Chem. Geol. **346**, 47 (2012).
[33]S. C. Glotzer, J. Non-Cryst. Solids **274**, 342 (2000).
[34]R. D. Shannon, Acta Cryst. A **32**, 751 (1976).
[35]A. Rahman, Phys. Rev. **136**, A405 (1964).
[36]M. S. Shell, P. G. Debenedetti, and F. H. Stillinger, J. Phys.: Condens. Matter **17**, S4035 (2005).
[37]C. A. Angell, Science **267**, 1924 (1995).
[38]H. Hasegawa, H. Ohata, H. Shibata, and Y. Waseda, High Temp. Mater. Process. **31**, 491 (2012).